

THE AEROSOL INDIRECT EFFECTS EXAMINED BY NUMERICALLY CALCULATED AEROSOLS

JP1.19

AND SATELLITE DERIVED CLOUDS

Kazuaki Kawamoto*¹, Tadahiro Hayasaka¹, Itsushi Uno² and Toshimasa Ohara³

1 Research Institute for Humanity and Nature, Kyoto, Japan

2 Kyushu University, Fukuoka, Japan

3 National Institute for Environmental Studies, Tsukuba, Japan

1. INTRODUCTION

Twomey (1977) first described the modification of cloud properties due to aerosols. Additional particles, which serve as cloud condensation nuclei (CCN), lead to a decrease in cloud particle size and an increase in the cloud optical depth of the constant liquid water content (LWC). This change is known as the aerosol indirect effect of the first kind, and the interaction between aerosols and clouds is one of the least understood processes related to climate change, including changes associated with global warming. The uncertainty of estimated global radiative forcing due to the aerosol indirect effect ranges from 0 to -2 W/m^2 , and the confidence level is “very low” (Ramaswamy 2001). It is therefore critical to accumulate research examples and provide a more reliable quantitative estimate of radiative forcing that accounts for the aerosol indirect effect.

* A number of studies have attempted to monitor this

* *corresponding author address:* Kazuaki Kawamoto, Research Institute for Humanity and Nature, Kyoto, Japan 603-8047; e-mail: kawamoto@chikyu.ac.jp

effect using satellite sensors and ground instruments, and observational techniques have steadily improved. For example, Han et al. (1994) used global data collected by the Advanced Very High Resolution Radiometer (AVHRR) to describe water cloud particle size. They found a distinct difference between land and ocean in cloud effective particle size. The number and chemical composition (e.g., hygroscopicity) of aerosols play important roles in determining cloud particle size. Feingold et al. (2003) used ground-based radiometric measurements and showed that the water cloud effective particle size decreases as the aerosol index increases. Nakajima et al. (2001) used AVHRR data to study the relationship between aerosols and water clouds over the global ocean. They showed that cloud effective particle sizes decrease, but the cloud optical depth increases, as the aerosol number density increases. Subsequently, Sekiguchi et al. (2003) described the behaviors of additional cloud properties (such as the cloud amount and cloud top temperature) using the aerosol number density based on the same AVHRR data set used by Nakajima et al. (2001). Breon et al. (2002) used Polarization and Directionality of the Earth's

Reflectances (POLDER) data to analyze aerosol–cloud relationships over land and ocean. They documented different rates of change in cloud effective particle size as a function of the aerosol indices for land and ocean.

In addition to global-scale analyses such as those mentioned above, regional studies targeting Asia are important due to high emission rates and locally focused aerosols. Chameides et al. (2002) compared model-simulated aerosol loading to cloud properties derived from International Satellite Cloud Climatology Project (ISCCP) data, with a focus over China. The ISCCP data included optical depth and showed that cloud optical depth positively correlated with aerosol loading. The relationship between aerosol loading and cloud amount, however, was not clear. They did not consider the behavior of cloud microphysical parameter because of limited ISCCP products.

Industrial production in China since the 1980s has quickly expanded following substantial political changes; consequently, various gaseous emissions have also rapidly increased (Streets and Waldhoff 2000). Heightened industrial activity has generated many aerosols and influenced air quality. China is therefore an ideal site to study the relationships between anthropogenic aerosols and clouds. As in the investigation by Chameides et al. (2002), this study examined the relationships between anthropogenic aerosols and clouds, including microphysics, to better understand human-induced effects on clouds over East Asia. Similar to the above-referenced papers (e.g., Nakajima et al. 2001, Breon et al. 2002, Sekiguchi et al. 2003), the present work also took a correlative approach to examine how aerosols affect the behaviors

of cloud properties, rather than pursuing the causative mechanisms of the aerosol indirect effect. Data used in this work included numerically simulated anthropogenic aerosol concentration and satellite-derived cloud properties. Both data types are described in the next section. A discussion of relationships between aerosols and clouds and the mechanisms involved follows. The last section provides the conclusions.

2. DATA

2.1. Anthropogenic aerosol concentration calculated from numerical model simulations

Satellite retrieval of aerosol properties has been considered difficult due to high reflectivity in visible wavelengths over land surfaces (Husar et al. 1997) and by cloud contamination in pixels. Therefore, this study used results from numerical simulations of anthropogenic aerosol concentration to examine the effects of human activities. Numerical simulations can provide long-term archives without gaps in data and can extract only anthropogenic components. The three-dimensional regional-scale chemical transport model used in this study was based on the Models-3 Community Multiscale Air Quality (CMAQ) modeling system released by the United States Environmental Protection Agency (Byun and Ching 1999) targeting East Asia (15–55°N, 90–135°E) with an 80 x 80-km² grid resolution. For vertical resolution, there were 14 layers in the *z*-coordinate system up to 23 km, with approximately seven layers within the boundary layer below 2 km. The meteorological fields were obtained

from the Regional Atmospheric Modeling System (RAMS) version 4.3 (Pielke et al. 1992; Cotton et al. 2003) using The National Center for Environmental Protection/National Center for Atmospheric Research (NCEP/NCAR) 2.5 x 2.5° reanalysis data sets for every 6 h; validation of this simulation was confirmed by Uno et al. (2005). The Statewide Air Pollution Research Center, version 99 (SAPRC-99) chemical mechanism, which includes 72 species and 214 reactions (Carter 2000) with an Euler Backward Iterative (EBI) solver, was adopted for gas phase chemistries in the CMAQ system used in this study. This CMAQ/RAMS Asia-scale modeling system was developed by Sugata et al. (2001) and Uno et al. (2005). Initial conditions for the chemical species modeled were based on the lowest values of the observed range. Boundary conditions for CMAQ were taken from monthly average output from a coupled global chemistry–climate model (Chemical AGCM for Study of Atmospheric Environment and Radiative Forcing: CHASER; Sudo et al. 2002a, b). For this CMAQ modeling system, anthropogenic emissions were obtained from an emission inventory for 1995 with a 0.5° x 0.5° resolution developed by the Frontier Research System for Global Change (FRCGC) and Research Institute for Humanity and Nature (RIHN) [<http://www.jamstec.go.jp/forsgc/research/d4/emission.htm>]. The fraction generated by biomass burning was sufficiently small so that the calculated aerosols could be considered largely “anthropogenic aerosols.” Non-methane volatile organic compounds (NMVOC) emissions were divided into the lumped-hydrocarbon SAPRC-99 categories using the method of Carter (2000). The five chemical species (sulfates, nitrates,

ammonia, and elemental and organic carbon) were considered to define the vertically integrated anthropogenic aerosol mass concentration M_a ($\mu\text{g}/\text{m}^2$) in this work. Respective aerosol particles were assumed to have the following three log-normal size distributions: an Aitken mode having a geometrical mean radius of 0.03 μm and geometrical standard deviation of 1.7, an accumulation mode having a geometrical mean radius of 0.3 μm and geometrical standard deviation of 2.0, and a coarse mode having a geometrical mean radius of 6.0 μm and geometrical standard deviation of 2.2.

Zhang et al. (2003) confirmed that simulated SO_4 concentrations agreed well with *in situ* observations in most cases but were overestimated in conditions such as high humidity in summer, weak rain, and fog. Simulations for 1995 were performed, and monthly mean values for January, April, July, and October were stored for this work.

2.2. Low cloud optical and microphysical properties observed using satellite data

Satellite data used in this work defined the cloud properties. The algorithm by Kawamoto et al. (2001) was used to retrieve cloud optical depths at visible wavelength τ , effective particle radius r_e (μm), and cloud top temperature T_c (K) warmer than 273 K. Cloud-reflected visible and near-infrared radiances and cloud-emitted infrared radiance were used. The retrieval assumed that solar radiance reflected by clouds at nonabsorbing visible wavelengths was a function of τ and that solar radiance reflected by clouds

at water-absorbing near-infrared wavelengths was a function of r_e near the cloud top (Nakajima and King 1990). The NCEP/NCAR reanalysis data provided humidity, pressure, temperature profiles, and surface temperatures to compute the cloud-emitted and surface-emitted thermal radiations and water vapor amounts above and under the cloud layer in the retrieval process.

Only low-level water clouds with cloud top temperatures warmer than 273 K may have occurred for the following reasons: most aerosols are within the lower part of the troposphere, and thus, aerosol interactions are more likely in low clouds than in other cloud types such as mid- and high-level clouds. Furthermore, this algorithm used the Mie scattering theory, which only applies to spheres in radiative transfer calculations. Super-cooled cloud particles below 273 K (until around 260 K) may also exist, but in an attempt to avoid potential bias in the correlations due to the inclusion of ice crystals, “clouds” hereafter refers to water clouds unless otherwise noted. According to Kawamoto et al. (2001), retrieval errors are generally 5–10% for τ and 10–15% for r_e , respectively.

The algorithm was applied to AVHRR Global Area Coverage (GAC) 3-channel radiances for 1995 (from NOAA-14), a year with relatively less influence from the Mt. Pinatubo eruption of 1991 and major El Niño Southern Oscillation (ENSO) events. The central wavelengths of channels 1, 3, and 4 of AVHRR were 0.64, 3.73, and 10.8 μm , respectively. East Asia (15–55°N, 90–135°E) was divided into 0.5° boxes to facilitate efficient processing. Each box contained 100 pixels. The segmented data were constructed daily for

the analysis period, and the one analyzed pixel had the median value of visible reflectivities among the cloudy pixels in each box. The cloud-screening procedure used visible and infrared radiances following the method of Kawamoto et al. (2001). The data processing incorporated the results by Iwabuchi and Hayasaka (2002), who showed that shadowing and three-dimensional effects are substantially reduced at viewing angles smaller than approximately 25°. Months that are representative of each season (January, April, July, and October) were analyzed, but temperature restrictions (warmer than 273 K) and solar zenith angle restrictions (smaller than 70°) in January yielded too few retrievals to determine statistical significance. Therefore, only the April, July, and October results were considered in this study. Calibration constants for channel 1 were adopted from Rao and Chen (1996) due to degradation after launch. Those for channels 3 and 4 were taken from internal black body instruments. The minimum value of visible radiance during the month in each grid box was converted to the ground reflectivity.

3. RESULTS AND DISCUSSION

Values of M_a and satellite-derived τ and r_e were correlated quantitatively in July as follows to examine cloud behaviors in relation to anthropogenic aerosols over East Asia. First, values of M_a were subdivided into bins. Cloud properties in the same geographical grid as the aerosol concentration were then collected, and an average and standard deviation of cloud properties for each M_a bin were computed. This comparison method has been used in previous studies (Nakajima et al.

2001; Breon et al. 2002; Kawamoto et al. 2004).

Figures 1 and 2 present the relationships of τ and r_e , respectively, for each M_a in July, with standard deviations shown. The two figures show that τ increased and r_e decreased as M_a increased. As mentioned previously, these tendencies are out of the range of retrieval uncertainty noted by Kawamoto et al. (2001). Such behaviors are consistent with the Twomey effect, i.e., the aerosol indirect effect of the first kind. As more aerosols are released to the atmosphere, more particles can serve as CCN and more cloud droplets are generated. In such situations, cloud droplet sizes will remain small because the constant LWC suggests that less water is available for each cloud droplet. The cloud optical depth, which is equivalent to the total surface area of cloud droplets, would increase due to the stronger effect of droplet number enhancement than that of particle size reduction. Other conditions such as aerosol hygroscopicity, dynamical processes, and water supply would also influence cloud properties in actual situations, as described in section 3.2. The SO_2 - r_e relationship reported by Kawamoto et al. (2004) in which SO_2 is converted to sulfate aerosols and then to CCN is analogous to the relationships proposed in this paper. Change rates of both τ and r_e with M_a became less steep for higher values of M_a (more than approximately $40 \mu\text{g}/\text{m}^3$), indicating saturation of the aerosol–cloud interaction in that region. A few previous studies have taken a similar correlative approach to the relationships between aerosols and clouds. For example, Chameides et al. (2002) used modeled anthropogenic aerosols and satellite-derived τ and found a comparable tendency to that in the present study. Chameides et al.

(2002) showed an overall positive correlation starting at a τ value of about 5 for an M_a of approximately $10 \mu\text{g}/\text{m}^3$ to a τ of approximately 12 for an M_a of about $50 \mu\text{g}/\text{m}^3$, with saturation for large M_a values.

Regarding r_e , Breon et al. (2002) found that aerosol indices were roughly 0.35–0.4 for heavily polluted regions such as the coastal and inland industrial regions of China and 0.08–0.12 for suburban regions. The values of r_e were approximately $7.7 \mu\text{m}$ and $8.3 \mu\text{m}$, respectively, for these regions. Geographically, such conditions corresponded to an r_e of approximately $9 \mu\text{m}$ for an M_a over $55 \mu\text{g}/\text{m}^3$ and an r_e of approximately 11 – $9.3 \mu\text{m}$ for an M_a of 10 to $20 \mu\text{g}/\text{m}^3$ in our case.

Breon et al. (2002) focused on the period from March to May using satellite-derived aerosol data that included both natural and anthropogenic origins.

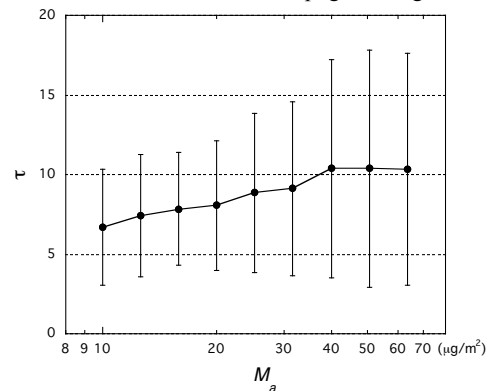


Fig. 1

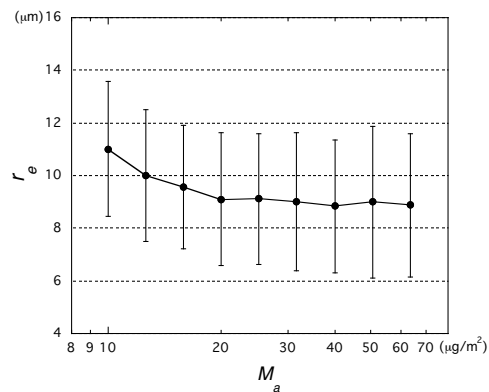


Fig. 2

Therefore, simple comparison of changing rates with our study is difficult. Differences in satellite sensors also raise problems. Rosenfeld and Feingold (2003), for example, have noted the differences in cloud sampling preferences between AVHRR and POLDER. The results of the present study are also difficult to compare with those by Nakajima et al. (2001) due to the type of satellite aerosol retrieval (including natural and anthropogenic aerosol origins) and because Nakajima et al. collected data only over the ocean. Among other satellite sensors, recent advancements in the Multiangle Imaging SpectroRadiometer (MISR) have led to unique monitoring at various angles that appear promising for land aerosol retrievals (Diner et al. 2001).

This study also investigated the relationship between M_a and the vertically integrated cloud droplet number N_c ($1/\text{cm}^2$), even though N_c , which was estimated from τ and r_e , was not an independent parameter. The following procedure was used to determine N_c . A log-normal size distribution with a variance of 0.35 was assumed for cloud droplets. The number density ($1/\text{cm}^3$) was calculated by integrating the size distribution; the number density was then divided by the extinction coefficient ($1/\text{cm}$) at the wavelength at which τ was observed to obtain the number density per optical depth ($1/\text{cm}^2$). Then N_c was determined as the product of this quantity and τ . As Fig. 3 presents, when M_a increased, N_c also increased. The vertically integrated aerosol particle number N_a , which was determined by integrating assumed size distributions with mass constants for species and M_a , was proportional to M_a ; therefore, a similar positive

relationship can be expected between N_a and N_c . This result can be considered to confirm one aspect of the Twomey effect (i.e., an increase in cloud droplet number with an increase in aerosol particle number).

Cloud property differences can be investigated with respect to differences in cloud top heights. Water clouds were divided into middle clouds (cloud top heights >3 km) and lower clouds (cloud top heights <3 km), and the same procedures as above were followed for both cloud types. Figures 4 and 5 show the relationships between τ and M_a , and r_e and M_a , for lower and middle clouds in July, respectively. Absolute values of both τ and r_e were generally larger for middle clouds. Cloud optical depth is a vertically integrated quantity, so higher clouds have a greater chance to become thicker. Larger cloud particle sizes in middle clouds arise from the smaller aerosol numbers at that altitude (note that this remote sensing method retrieves r_e near the cloud top), as indicated by Kawamoto et al. (2001). Increases in τ and decreases in r_e and M_a for both cloud types were similar to those in Figs. 4 and 5 and also consistent with the Twomey effect. However,

geographical patterns between M_a and cloud properties in April over southern China (around

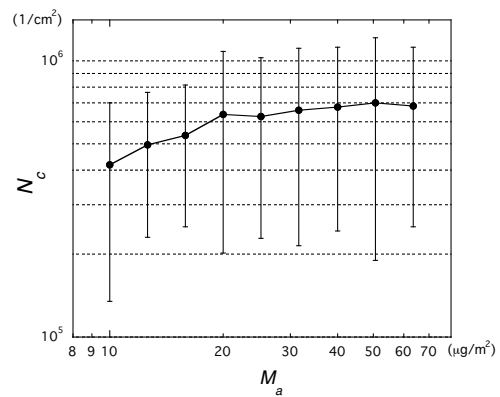


Fig.3

22–32°N, 105–120°E) were not as comparable. This suggests that not only the particle processes considered here but also dynamic processes should be examined because this area is rather convective.

4. Conclusions

This paper has discussed the relationships between anthropogenic aerosols and low-level water clouds to try to better understand the aerosol indirect effect over East Asia. Results from numerical simulations yielded the anthropogenic aerosol concentration. Satellite-derived products yielded information on low-level water cloud properties. Comparisons of monthly means for aerosols and clouds showed that τ increased and r_e decreased as M_a increased. Such tendencies were consistent with the Twomey effect, which describes how aerosols affect cloud properties. This behavior is analogous to the SO_2 – r_e relationship described by Kawamoto et al. (2004). Nevertheless, comparisons of M_a with τ in April and October would suggest the importance of dynamic effects on cloud formation and maintaining processes that were not intensively discussed in this work. Analyses that combine dynamical processes will be the subject of further study. Values of N_c that were calculated from τ and r_e also increased as M_a increased. This result also agreed with the Twomey effect by indicating that additional aerosols generated more cloud droplets. A comparison of M_a with lower and middle clouds revealed similar tendencies to the previous case (i.e., total water cloud case), but differences in r_e (i.e., larger for middle and smaller for lower clouds) reflected the vertical profile

of aerosol numbers. However, differences in τ (i.e., thicker for middle and thinner for lower clouds) might have been influenced by the vertical extent. These findings were obtained with cloud microphysical information that was unavailable to Chameides et al. (2002).

The changing rates of cloud properties with M_a are important not only to describe the phenomena but also for parameterizations in numerical model applications. More studies involving both satellite observations and numerical modeling are needed to validate these rates and make them more robust. There are some papers that support the conclusions of this study. Breon et al. (2002), for example, stated that “there is a clear physical process that predicts such a decrease [of cloud particle size]...this observed correlation can be

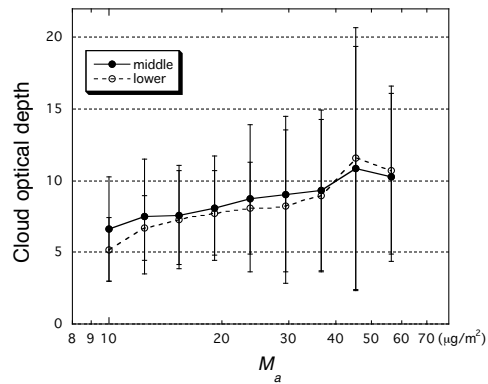


Fig.4

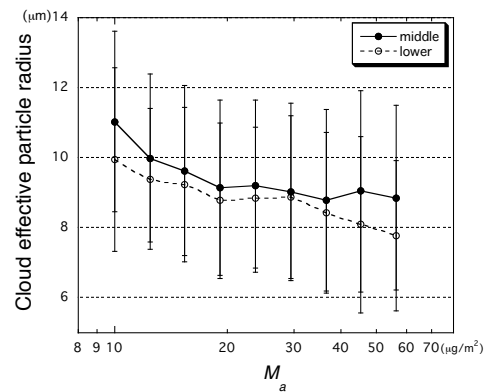


Fig.5

interpreted as a causal connection.” Although we showed several phenomena that were consistent with the effect suggested by Twomey, the correlative analysis that we used here does not guarantee a causal relationship between the two quantities. Therefore, we must exercise caution in discussing the robust causality of the aerosol indirect effect and must continue to accumulate research examples based on observations and modeling.

Acknowledgements

K.K. was supported by Special Coordination Funds for Promoting Science and Technology of Japan and the RIHN research project 2-1 (Emissions of Greenhouse Gases and Aerosols and Human Activities in East Asia). We thank Dr. S. Satake for his valuable comments. Some ISCCP cloud products were used for comparison purposes.

References

- Breon, F.-M., D. Tanre, and S. Generoso, 2002: Aerosol effect on cloud droplet size monitored from satellite. *Science*, **295**, 834–838.
- Byun, D.W., and J.K.S. Ching, 1999: Science algorithms of the EPA Models-3 community multi-scale air quality (CMAQ) modeling system, NERL, Research Triangle Park, NC, EPA/600/R-99/030.
- Carter, W.P.L., 2000: Documentation of the SAPRC-99 chemical mechanism for VOC reactivity assessment. Final report to California Air Resource Board. Contract No. 92-329 and 95-308.
- Chameides, W.L., C. Luo, R. Saylor, D.G. Streets, Y. Huang, M. Bergin, and F. Giorgi, 2002: Correlation between model-calculated anthropogenic aerosols and satellite-derived cloud optical depths: Indication of indirect effect? *J. Geophys. Res.* **107**, doi:10.1029/2000JD000208.
- Cotton, W.R., R.A. Pielke, and R.L. Walko, 2003: RAMS 2001: Current status and future directions. *Meteorol. Atmos. Phys.* **82**, 5–29.
- Diner, D. J., W. A. Abdou, C. J. Bruegge, J. E. Conel, K. A. Crean, B. J. Gaitley, M. C. Helmlinger, R. A. Kahn, J. V. Martonchik, S. H. Pileorz and B. N. Holben, 2001: MISR aerosol optical depth retrievals over southern Africa during the SAFARI-2000 dry season campaign. *Geophys. Res. Lett.* **28**, 3127-3130.
- Feingold, G., W.L. Eberhard, D.E. Veron, and M. Previdi, 2003: First measurements of the Twomey indirect effect using ground-based remote sensors, **30**, 1287, doi:10.1029/2002GL016633.
- Han, Q., W. B. Rossow, and A.A. Lacis, 1994: Near-global survey of effective droplet radii in liquid water clouds using ISCCP data. *J. Climate.* **7**, 465-497.
- Husar, R.B., J.M. Prospero, and L.L. Stowe, 1997: Characterization of tropospheric aerosols over the oceans with the NOAA Advanced Very High

- Resolution Radiometer optical thickness operational product. *J. Geophys. Res.* **102**, 16889–16909.
- Iwabuchi, H. and T. Hayasaka 2002, Effects of cloud horizontal inhomogeneity on the optical thickness retrieved from moderate-resolution satellite data, *J. Atmos. Sci.* **59**, 2227-2242
- Kawamoto, K., T. Nakajima, and T. Y. Nakajima, 2001: A global determination of cloud microphysics with AVHRR remote sensing. *J. Climate*. **14**, 2054–2068.
- Kawamoto, K., T. Hayasaka, T. Nakajima, D.G. Streets, and J.-H. Woo, 2004: Examining the aerosol indirect effect over China using an SO₂ emission inventory. *Atmos. Res.* **72**, 353–363.
- Kawamoto, K., In press: Relationships between cloud properties and precipitation amount over the Amazon basin. *Atmos. Res.*
- Nakajima, T. and M. D. King, 1990: Determination of the optical thickness and effective radius of clouds from reflected solar radiation measurements. Part I: theory. *J. Atmos. Sci.*, **47**, 1878-1893.
- Nakajima, T., A. Higurashi, K. Kawamoto, and J. E. Penner, 2001: A possible correlation between satellite-derived cloud and aerosol microphysical parameters. *Geophys. Res. Lett.*, **28**, 1171-1174.
- Pielke, R.A., W.R. Cotton, R.L. Walko, C.J. Tremback, W.A. Lyons, L.D. Grasso, M.E. Nicholls, M.D. Moran, D.A. Wesley, T.J. Lee, and J.H. Copeland, 1992: A comprehensive meteorological modeling system—RAMS. *Meteorol. Atmos. Phys.* **49**, 69–91.
- Ramaswamy, V. 2001: Radiative forcing of climate change, pp. 349–416. *Climate Change 2001: The Scientific Basis*. J. T. Houghton et al., eds., Cambridge University Press, Cambridge. 884 pp.
- Rao, C.R.N. and J. Chen, 1996: Post-launch calibration of the visible and near-infrared channels of the Advanced Very High Resolution Radiometer on the NOAA-14 spacecraft. *Int. J. Remote Sens.* **17**, 2743–2747.
- Rosenfeld, D. and G. Feingold, 2003: Explanation of discrepancies among satellite observations of the aerosol indirect effects. *J. Geophys. Res.*, **30**, No. (14), 1776, doi:10.1029/2003GL017684.
- Sekiguchi, M., T. Nakajima, K. Suzuki, K. Kawamoto, D. Rosenfeld, S. Mukai, and I. Sano, 2003: A study of the direct and indirect effects of aerosols using global satellite data sets of aerosol and cloud parameters, *J. Geophys. Res.* **108**, doi:10.1029/2002JD003359.
- Streets, D., and Waldhoff, S.T., 2000. Present and future emissions of air pollutants in China: SO₂, NO_x, and CO. *Atmos. Environ.* **34**, 363_374.
- Streets, D.G., K.F. Yarber, J.-H. Woo, and G.R. Carmichael, 2003: Biomass burning in Asia: Annual

- and seasonal estimates and atmospheric emissions. *Glob. Biogeochem. Cycles* **17**, doi:10.1029/2003GB002040.
- Sudo, K., M. Takahashi, J. Kurokawa, and H. Akimoto, 2002a: CHASER: A global chemical model of the troposphere-1. Model description. *J. Geophys. Res.* **107**, doi:10.1029/2001JD001113.
- Sudo, K., M. Takahashi, and H. Akimoto, 2002b: CHASER: A global chemical model of the troposphere-2. Model results and evaluation. *J. Geophys. Res.* **107**, doi:10.1029/2001JD001114.
- Sugata, S., D. Byun, and I. Uno, 2001: Simulation of sulfate aerosol in East Asia using Models-3/CMAQ with RAMS meteorological data, pp. 267–275. In S.-E. Gryning and E. Schiermeier, eds., *Air Pollution Modeling and Its Application XIV*. Plenum Press, New York.
- Torres, O., P.K. Bhartia, J.R. Herman, A. Sinyuk, and B. Holben, 2002: A long term record of aerosol optical thickness from TOMS observations and comparison to AERONET measurements. *J. Atmos. Sci.* **59**, 398–413.
- Twomey, S., 1977: The influence of pollution on the shortwave albedo of clouds. *J. Atmos. Sci.* **34**, 1149–1152.
- Uno, I., T. Ohara, S. Sugata, J. Kurokawa, N. Furuhashi, K. Yamaji, N. Tanimoto, K. Yumimoto, and M. Uematsu, 2005: Development of RAMS/CMAQ Asian scale chemical transport modeling system. *J. Jpn. Soc. Atmos. Environ.* **40**, 148–164.
- Zhang, M.G., I. Uno, G.R. Carmichael, H. Akimoto, Z.F. Wang, Y.H. Tang, J.-H. Woo, D.G. Streets, G.W. Sachse, M.A. Avery, R.J. Weber, and R.W. Talbot, 2003: Large-scale structure of trace gas and aerosol distributions over the western Pacific Ocean during the Transport and Chemical Evolution Over the Pacific (TRACE-P) experiment. *J. Geophys. Res.* **108**, doi:10.1029/2002JD002946.

Figure captions

Fig. 1. Relationship between M_a and t in July 1995.

Fig. 2. Relationship between M_a and r_e in July 1995.

Fig. 3. Relationship between M_a and N_c in July 1995.

Fig. 4. Relationship between M_a and τ for middle and lower clouds in July 1995.

Fig. 5. Relationship between M_a and r_e for middle and lower clouds in July 1995.